

615306
P. 11

DESIGN CONSIDERATIONS OF ISTAR HYDROCARBON FUELED COMBUSTOR OPERATING IN AIR AUGMENTED ROCKET, RAMJET AND SCRAMJET MODES

Dean Andreadis, Alan Drake, Joseph L. Garrett, Christopher D. Gettinger, Stephen S. Hoxie
Pratt & Whitney Space Propulsion
West Palm Beach, FL

(dean.andreadis@pw.utc.com, alan.drake@pw.utc.com, joseph.garrett@pw.utc.com,
christopher.gettinger@pw.utc.com, stephen.hoxie@pw.utc.com)

Abstract

The development and ground test of a rocket-based combined cycle (RBCC) propulsion system is being conducted as part of the NASA Marshall Space Flight Center (MSFC) Integrated System Test of an Airbreathing Rocket (ISTAR) program. The eventual flight vehicle (X-43B) is designed to support an air-launched self-powered Mach 0.7 to 7.0 demonstration of an RBCC engine through all of its airbreathing propulsion modes — air augmented rocket (AAR), ramjet (RJ), and scramjet (SJ). Through the use of analytical tools, numerical simulations, and experimental tests the ISTAR program is developing and validating a hydrocarbon-fueled RBCC combustor design methodology. This methodology will then be used to design an integrated RBCC propulsion system that produces robust ignition and combustion stability characteristics while maximizing combustion efficiency and minimizing drag losses. First order analytical and numerical methods used to design hydrocarbon-fueled combustors are discussed with emphasis on the methods and determination of requirements necessary to establish engine operability and performance characteristics.

Introduction

The Advanced Space Transportation Program (ASTP) focuses technology development in four investment areas as described in References 1 and 2. One investment area is the hypersonic (3rd Generation Reusable Launch Vehicle [3GRLV]) system with the goals to make future transportation safer, more reliable, and significantly less expensive than today's missions. Under the ASTP, NASA MSFC is conducting the ISTAR project to develop and ground test an RBCC propulsion system and potentially conduct a flight test experiment.

NASA MSFC has assembled a team consisting of U.S. Government and industry participants, to conduct the development and ground test of the RBCC propulsion system. The U.S. Government team includes participants from several NASA centers: Dryden Flight Test Center, Glenn Research Center, Langley Research Center, MSFC and Stennis Test Center. The primary industry team member is the Rocket-Based Combined Cycle Consortium (RBC³), which includes Boeing Rocketdyne, United Technologies Pratt & Whitney (UTC P&W), and Gencorp Aerojet. In addition to the RBC³ members, the ISTAR project is also supported by Boeing for vehicle-level studies.

Significant advancements in vehicle systems and scramjet propulsion have been accomplished under several previous and current programs. In particular, the National Aerospace Plane (NASP) program³ and NASA's Hyper X (X-43A) program⁴ have significantly advanced the technologies required for vehicles using hypersonic airbreathing propulsion systems. As part of the Air Force Hypersonic Technology (HyTech) program, the U.S. Air Force is developing the technologies necessary to demonstrate the operability, performance, and struc-

tural integrity of liquid hydrocarbon-fueled scramjet engines.^{5,6} Under the Hypersonic Scramjet Engine Technology (HySET) program, a full-scale, flight-weight, fuel-cooled engine (Ground Demonstration Engine [GDE-1]) is being tested at GASL's Leg VI facility.⁷ The GDE-1 will prove to be a promising candidate for future scramjet applications and set the groundwork for such applications as X-43C and ISTAR programs. The state of the art of RBCC propulsion has been advanced by such projects as Advanced Reusable Transportation Technologies (ARTT). The aforementioned programs have provided analytical methods and demonstrated performance for different modes of engine operation through ground engine testing and technology development necessary for the conceptual design of the RBCC propulsion system.

The conceptual design of the flight test engine (FTE) of the RBCC propulsion system and the X-43B demonstrator is being developed under Phase I of the ISTAR project. At the conclusion of Phase I, the requirements of the engine design will be translated into a suitable specification for a sophisticated ground test engine, which will be designed to reduce the risks inherent in powerplant development through the demonstration of each significant propulsion mode. Phase II will derive the requirements to design, fabricate, and test an RBCC engine for ground test demonstrator engine (GTDE) simulation both at sea-level static (SLS) and at simulated altitude conditions. The X-43B flight demonstration will then begin the preliminary design of an engine/vehicle system that takes into account the lessons learned from the ground test program and follows through to construction and flight test of the X-43B. The FTE will be capable of powering a flight demonstrator vehicle from launch off a carrier air-

craft (at Mach 0.7) up to scramjet speeds of Mach 7.0.

This paper focuses on the design approaches and first order analytical and numerical considerations of the hydrocarbon-fueled combustor operating in the various modes required for engine operability and performance of an RBCC-powered system.

Vehicle Concept and Mission Profile

Airbreathing vehicle systems feature a high level of integration between airframe and engine. Therefore, under the ISTAR project, initial demonstrator vehicle and engine design and integration is being performed, including three degree-of-freedom trajectory analyses to ensure vehicle mission closure and define propulsion requirements. Engine and aerodynamic performance, structure, weight, systems, packaging, and thermal management are traded against each other to develop a balanced vehicle solution that meets mission requirements and thus, defines a closed configuration.⁸

Figure 1 depicts the X-43B vehicle design featuring a planform that includes a wing-body concept with a canard. It is to be constructed of a conventional metallic structure that is protected by an advanced reusable thermal protection system. The design will feature only incremental technology improvements over the preceding X-43A and X-43C demonstrator vehicles, reflecting the program's focus on propulsion system development.

The mission profile of the X-43B vehicle is designed to facilitate the demonstration of all significant RBCC propulsion modes. Following release from a carrier aircraft at approximately Mach 0.7

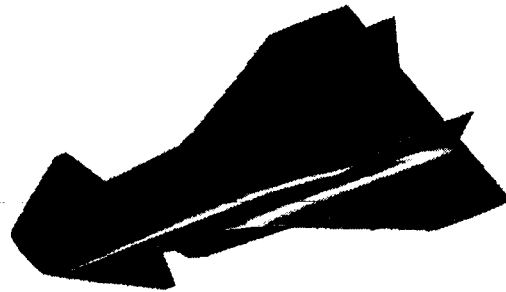


Figure 1. X-43B Vehicle Configuration

and 35,000 ft, the vehicle free-falls for a few seconds before starting engine operation. The vehicle then accelerates at a moderate flight path angle to reach a dynamic pressure of approximately 2000 psf by approximately Mach 4, maintaining constant dynamic pressure from that point until reaching Mach 7 and 90,000 ft before shutting down the engines and gliding back for reuse (Figure 2).⁹ During the acceleration phase, the propulsion system transitions through three basic propulsion modes: AAR, RJ, and SJ.

Engine Concept and Operational Modes

A schematic of an RBCC component arrangement is presented in Figure 3. Several individual flowpaths, each separated by splitters, comprise the complete propulsion system. The RBCC propulsion flowpath consists of an external vehicle forebody, internal inlet, an isolator section, integrated rockets, a combustor section, and an internal nozzle with a single expansion ramp aft body.

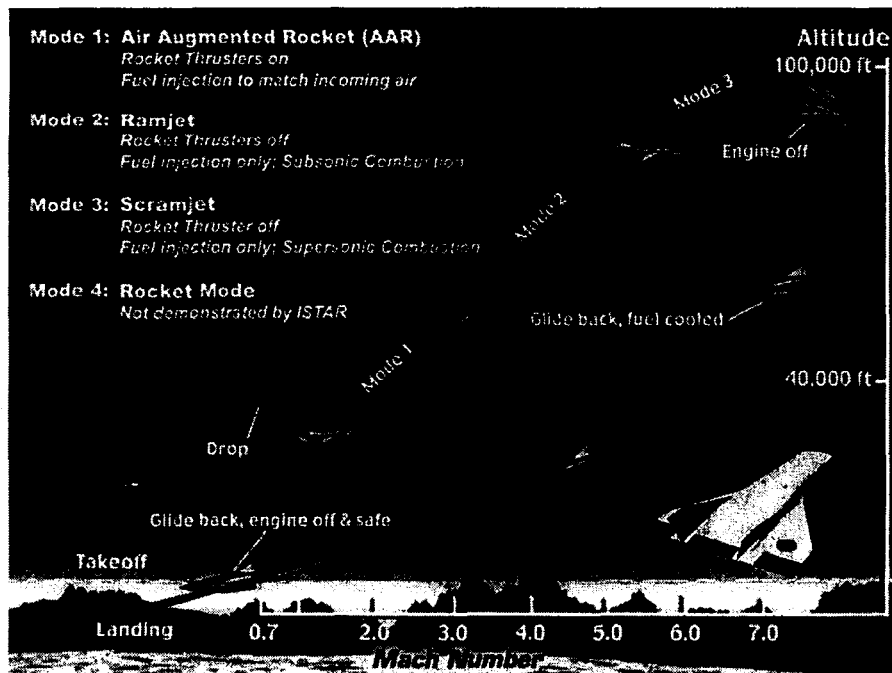


Figure 2. X-43B/ISTAR Mission Profile

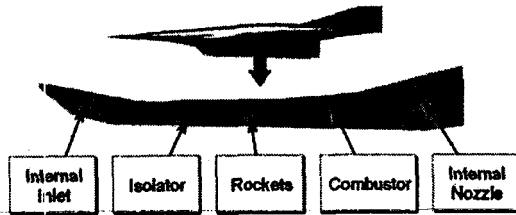


Figure 3. E200 ISTAR Engine Configuration

The vehicle forebody has been synergistically designed with the internal inlet and cowl flap to provide the required mass capture and aerodynamic contraction ratio at maximum inlet efficiency. The isolator section is incorporated to prevent combustor-inlet interactions and sized to accommodate the maximum precombustion pressure rise over the projected flight envelope. The RBCC engine incorporates a fixed-geometry, thermally-throated dual-mode ramjet/scramjet combustor designed with consideration of AAR and RJ/SJ performance and operability requirements. It is capable of operation over the entire flight envelope. The internal nozzle has been synergistically integrated with the combustor and vehicle aft body to maximize thrust potential and

balance aerodynamic and propulsive moments. Design guidelines and models have been developed to define mass capture, contraction ratio limits, shock strength limits for boundary layer interaction, isolator length requirements, fuel injector mixing and drag characteristics, combustor area ratio/distribution, and nozzle thrust coefficients. These models are used in the system analysis¹⁰ to address engine operability and performance.

During the acceleration phase, the RBCC propulsion system transitions through three basic propulsion modes: AAR, RJ, and SJ as shown in Figure 4.⁹ The AAR mode consists of two distinct submodes of operation, ejector rocket (ER) mode with inlet subcritical (i.e., unstarted) and AAR mode with inlet supercritical (i.e., started). In the ER mode of operation, rocket thrusters operate and serve to induce secondary airflow into the subcritical inlet through an ejector mechanism. Additional fuel is injected based on the secondary airflow entrainment, and therefore, modest supplemental combustion of this additional fuel with air occurs during this phase of the mission, increasing thrust and efficiency over that of the bare rocket.

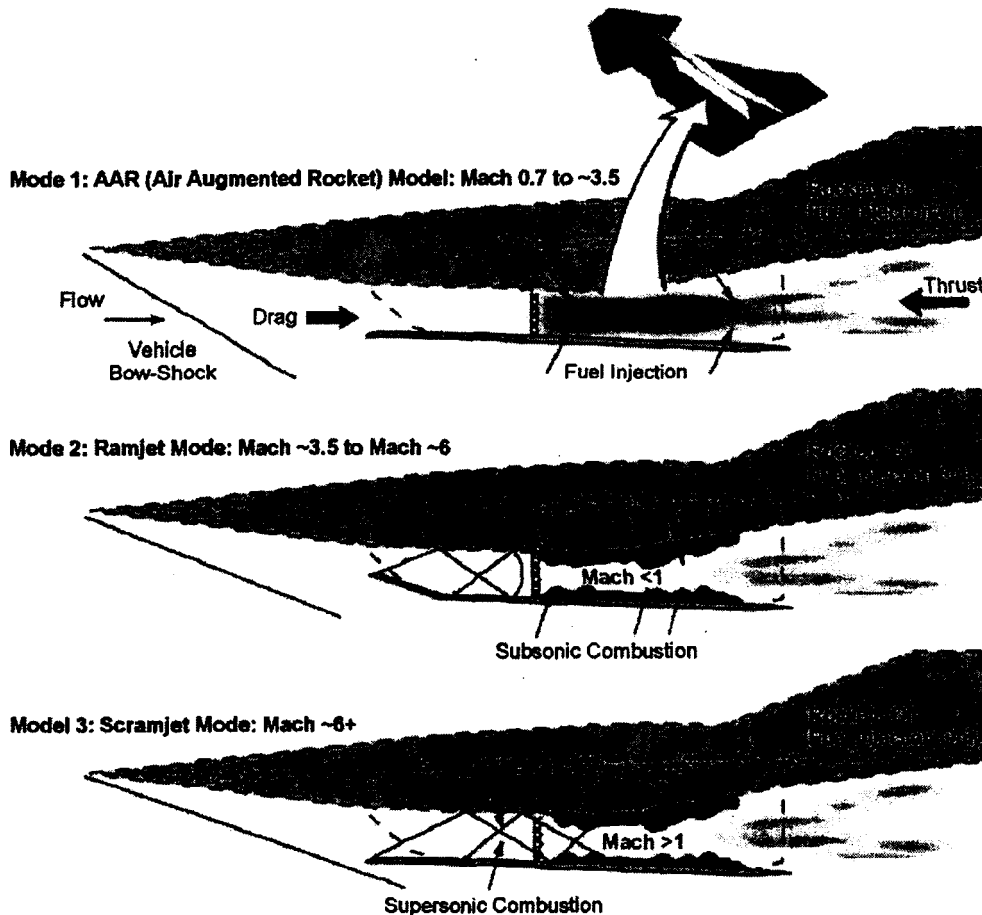


Figure 4. ISTAR Engine Operating Modes

As the vehicle continues to accelerate, the inlet becomes supercritical or started (Mach 2+). The ingested airflow is then determined by the inlet geometry rather than the rocket operation. The greatly increased secondary airflow is fueled through dedicated injector sites to achieve maximum thrust augmentation during this portion of the mission. The rocket plume serves to pilot the secondary combustion process. The fuel schedule is set by the maximum amount of energy that can be added to the airstream without exceeding the pressure rise capability of the isolator (causing the inlet to unstart).

The AAR to RJ mode transition (Mach 3 to 4) occurs when the rocket thrusters are throttled back and ultimately cutoff while the secondary airstream is fueled to produce the maximum sustainable pressure rise in the isolator for RJ operation. Fuel is staged as required to maintain inlet start conditions. The final mode of operation, SJ, occurs as the vehicle approaches flight Mach 6+ and the isolator and combustion processes throughout the engine are supersonic, even when all fuel is staged to the furthest forward fuel injectors.

Combustor Design Methods and Considerations

The ISTAR project has employed a multidisciplinary design process in designing the RBCC propulsion system to operate over the Mach range from 0.7 to 7.0. The process considers engine and vehicle aerodynamic performance, mass properties and fuel system, packaging, and thermal management and is iterated until the vehicle arrives at a closed configuration (i.e., a configuration that can perform the desired mission with the available fuel volume). One of the steps in the multidisciplinary design process is the definition of combustor/injector design and associated performance. First-order analyses and design methods are used to evaluate combustor configuration and to establish their dimensions for design purposes. The combustor design methods enable the assessment of secondary air entrainment and thrust

augmentation, flame stability and propagation, fuel penetration and spreading characteristics, base pressurization and drag, mixing, and combustion efficiency. The combustor design methods are presented in Figure 5 along with interactions occurring with other engine components.

The mission performance requirements (delta velocity and range) and vehicle characteristics (drag, empty weight, and propellant volume and density) are used to determine thrust targets through first-order trajectory simulation. These thrust targets, particularly in the ramjet and scramjet regimes, define the engine capture area given a thrust per unit airflow based on prior experience. Forebody and inlet design geometric characteristics are dictated by design Mach number, vehicle integration, and internal inlet operability issues. Internal inlet convergence is set to minimize boundary layer separation. Inlet operability is assessed initially using lower fidelity tools and is subsequently substantiated through higher fidelity analyses, such as three-dimensional (3-D) computational fluid dynamics (CFD).

Transonic vehicle drag characteristics and sufficient low-speed acceleration during ER and AAR modes of operation dictate bare rocket thrust to meet mission requirements. Rocket thruster integration drives base area requirements, lateral distribution, and maximum perimeter exposure to secondary airflow as a function of rocket critical parameters such as chamber pressure, throat area, and nozzle expansion ratio. Once inlet exit stream thrust averaged conditions, boundary layer properties, and rocket lateral distribution are defined, the isolator model is employed to map pressure rise capability (as a function of throat Mach number) for a specified geometry. Combustor pressure rise demand is then compared to the maximum pressure rise capability the isolator can supply to establish isolator length and fuel staging requirements.

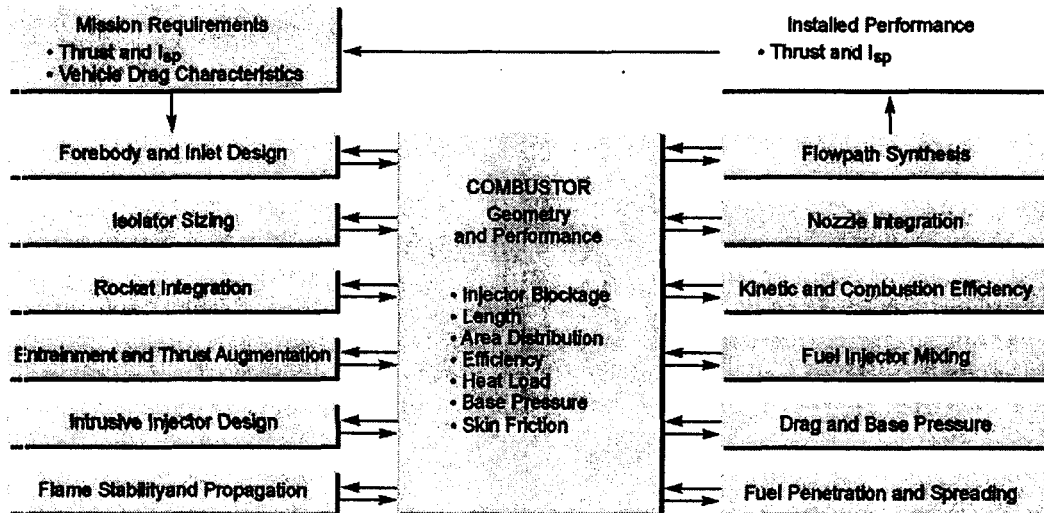


Figure 5. Combustor Design Model Features

An additional consideration in rocket integration is the impact on high-speed (RJ and SJ) combustor performance. In particular, the amount of base area introduced into the flowpath due to the rocket integration must be controlled. While some base area is desirable to aid in flameholding, a large amount of base area in the flowpath will result in excessive flowpath drag during scramjet operation. Because the rocket base area is used for flameholding in RJ and SJ modes of operation, the impact of its integration into the flowpath on fuel injection location is also critical. Injector locations drive the fuel mixing and combustion characteristics in ER, AAR, RJ, and SJ modes of operation and mode transition.

Penetration and spreading requirements for the injectors are set by many considerations. Primary and secondary injector sizing and spacing is set to accommodate intrusive injector lateral distribution, combustor entrance profiles, fuel staging, and variations in fuel properties along the described mission. Upon establishing fuel penetration and spreading characteristics, mixing models are employed based on critical parameters such as injector penetration, duct height, pressure ratio across the injectors, spacing, jet diameter, and equivalence ratio to determine combustor length requirements.

Another critical performance driver in the RBCC engine is the combustor area distribution, which must be sized in a fashion to balance low speed (ER and AAR) and high speed (RJ and SJ) combustion requirements. Combustor area distribution and length must be sufficient to accommodate AAR thrust augmentation and the desired equivalence ratio at combustion efficiency set by mission requirements while minimizing kinetic effects during RJ and SJ modes and mode transitions (AAR to RJ and RJ to SJ) without excessive combustor inlet interactions. Once mixing efficiency and combustor area distributions are established, kinetic analysis is employed to ultimately determine combustion efficiency. Kinetic effects are more pronounced during RJ and SJ operation and therefore tend to bound the rate of combustor divergence in the near field of the combustor, while higher combustor divergence is preferred for AAR operation.

Synergistic internal nozzle and aft body integration is accomplished by selecting the appropriate final combustor angle and initial and final body side arc surface angles along with cowl angle and length to maximize installed propulsion performance and vehicle volume. In general, improvements in net propulsive force in AAR mode result in deterioration of net propulsive force in RJ and SJ modes, and conversely.

The thermally- and power-balanced airbreathing RBCC engine environment provides unique thermal challenges. Considerations must be given to the flowpath environment (maximum pressure, temperature, and heat flux) and corresponding available sec-

ondary fuel flow rates across the entire mission, and particular attention should be given to AAR and SJ modes of operation before selecting design points. Once engine flowpath lines and environment are established, heat flux profiles are calculated. The integrated heat flux provides combustor, and ultimately, engine heat loads.

The flowpath synthesis process involves integrating the forebody, inlet, isolator, combustor and nozzle components into one balanced nose-to-tail flowpath. Installed propulsion performance is then generated in cooperation with the vehicle designer in keeping with an agreed-upon force accounting system. Propulsion performance (thrust, lift, and moments) is integrated with vehicle aerodynamic forces to develop trimmed aerodynamic performance through a suitable three degree-of-freedom trajectory analysis. The air vehicle and propulsion system designs are fully integrated so that the resulting propulsion system objectives would enable the air vehicle to demonstrate the mission system goals.

Of all the combustor design considerations presented in Figure 5, five were chosen to discuss further in detail in this paper: Entrainment and Thrust Augmentation, Flame Stability and Propagation, Fuel Penetration and Spreading, and Combustor Thrust Potential and Engine ISP Optimization. Each of these items is discussed in detail in the following four sections. The Combustor Thrust Potential and Engine I_{sp} Optimization section addresses combustor considerations and interactions such as intrusive injector design, fuel injector mixing, drag and base pressure and kinetics and combustion efficiency.

Entrainment and Thrust Augmentation

In the ER and AAR mode, air entrainment and thrust augmentation are the primary measure of engine performance. However, while entrainment of a larger amount of air increases the potential for higher efficiency, this efficiency is not always realized due to associated losses incurred in the air entrainment process. Proper tracking of these losses is key to determining both the amount of air entrained (in ER mode), and the resulting thrust created by the combustion of fuel with the entrained air.

For the ER mode (where the inlet is subcritical), the amount of air entrained into an RBCC engine by the rocket ejector system is fundamentally limited by either the ejector pumping limit or a by a mixed flow choking limit as shown in Figure 6. The ejector pumping limit is determined by the amount of momentum transfer from the primary (rocket) stream to the secondary (air) stream. Momentum is transferred from the primary to secondary streams by changing of the streamtube areas when the two streams interact (due to a stream pressure differential), and by work transfer caused by shear forces between the primary and secondary streams (due to a stream velocity differential).

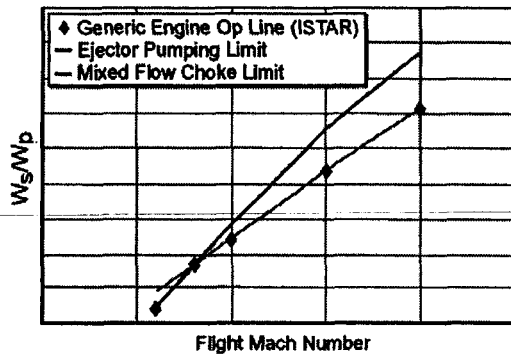


Figure 6. Physical Limits to Air Entrainment and Thrust Augmentation

A myriad of models have been proposed to characterize the ejector pumping limit, the simplest of which are ideal models like the Fabri model¹¹ and the compound compressible flow model proposed by Bernstein, et. al.¹² These ideal models are simple to implement and easily understood. However, they do not account for the impact of shear forces (or any other losses) between the primary and secondary streams, which is the only mechanism for momentum transfer between the two streams when the rocket exit flow and incoming air flow are pressure matched.

The mixed flow choking limit can be encountered as the rocket and air streams (and any supplemental fuel streams) are combined, mixed and combusted. In general, an RBCC engine will be limited at low freestream total pressures by the ejector pumping limit, and will transfer to the mixed flow choking limit as the freestream total pressure increases.

Since the major drivers to ER performance are a balance of high entrainment and efficient flow processing through the ejector and mixer, a way to characterize the entrainment and mixing efficiency of an ejector is required, so that ejector performance can be compared between candidate systems. One such measure of efficiency is the Stagnation Momentum Exchange Effectiveness (SMEE) proposed in Refer-

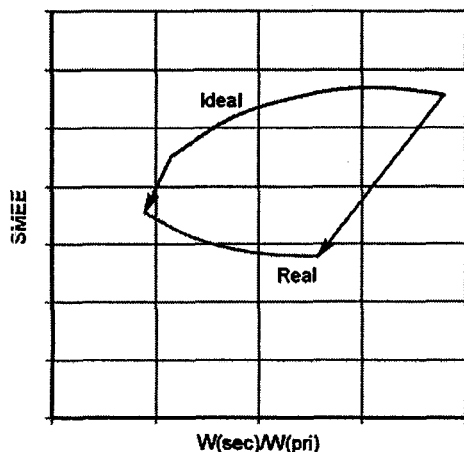


Figure 7. Ejector Maps (Typical Pumping Characteristics)

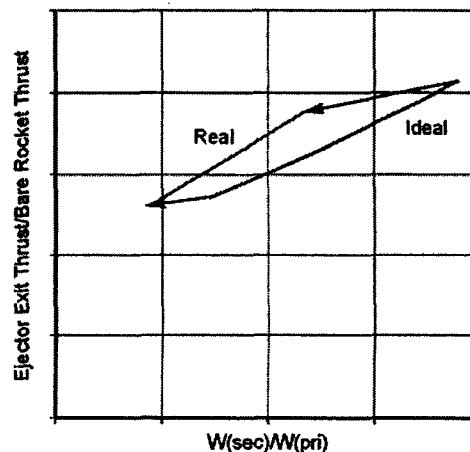
ence¹³. The SMEE parameter defines ejector and mixer system efficiency in terms of total conditions at the mixer exit as compared to the total conditions existing in the primary and secondary streams before the two streams come into contact.

To underscore the importance of properly accounting for losses in the ejector and mixer processes, ejector performance (in terms of SMEE and thrust ratio) for ideal and real engines are shown in Figure 7. The results in Figure 7 verify that inclusion of losses into the ejector system is crucial to predicting proper overall engine performance.

As the engine transfers from ER to AAR mode (i.e., the inlet starts), the amount of flow ingested into the engine is no longer controlled by the rocket ejector system. The flight condition at which the inlet starts may be influenced by the rocket ejector system. In fact, if the rocket exit pressure is too high, the ejector system may act as effective blockage in the flowpath and cause the inlet to remain subcritical until a higher free-stream Mach number has been achieved. Therefore, maximum overall engine system performance may dictate that the ejector rockets be throttled back to allow the inlet to start at a lower flight Mach number.

Recirculation Zone Mass Exchange and Flame Stability

Hydrocarbon fuel was chosen for the ISTAR program because of its inherent thermal stability and demonstrated ability to provide a sizable endothermic heat sink capability. Owing to the long ignition delay associated with combustion of hydrocarbon fuels, a robust ignition and combustion-piloting source is required. The critical component that controls both the flameholding and flame propagation characteristics is the mass exchange rate between the flameholder recirculation zone and the combustor core flow. Critical parameters that drive the flameholder blowout limit are the fuel/air equivalence ratio, ignition and residence and reaction times in the flameholder recirculation zone. The transverse velocity component and ultimately mass exchange



between the recirculation zone and primary axial flow can be characterized by the Winterfeld model.¹⁴ Alternative models such as one-dimensional (1-D) momentum balance over the recirculation with a base pressure model can determine mass exchange ratio as described in Reference 15. The momentum balance model requires that the forces acting on the flameholder be equal to the pressure integral over the wake separation bubble and the drag created by the turbulent mass exchange with the core flow. In this model the velocity of the mass entrained from the recirculation is assumed to be $1/3$ of the core flow velocity.

The stability of the flame in the base region of the intrusive injectors can be assessed in terms of a blowoff parameter, P_{bo} or stability correlation parameter¹⁶ defined as follows:

Equation 1

$$P_{bo} \propto \left(\frac{U}{d}\right) \left(\frac{d}{d_e}\right) \left(\frac{P_o}{P}\right) \left(\frac{1000}{T}\right)$$

Where:

U is the velocity of the flow at the location of the flame stabilizer

d is a characteristic dimension (e.g., height or diameter)

P_o is reference static pressure

T is total temperature.

This parameter was originally developed based on subsonic combustion data for hydrocarbon fuel-air combustion. On that basis, the use of total temperature in Equation 1 may be justified. Note however, that in subsonic flow (as opposed to supersonic flows) processes occurring downstream from the flame stabilizer lip affect upstream conditions. The quantities of significance in flameholder stability, as understood by the authors, are the conditions immediately adjacent to and upstream from, the flame stabilizer. On the basis of data acquired during the course of the HySET program,^{5,6} stability parameter levels were calculated for test data acquired during the course of that experimental effort. Regions of the stability data are shown in Figure 8 and are compared with a stability curve for kerosene, extracted from Reference 16.

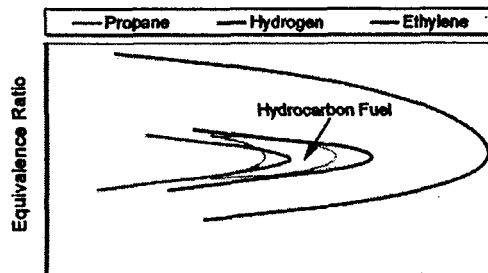


Figure 8. Flame Stability Correlation

Fuel Penetration and Spreading Characteristics

Methods for predicting the fuel distribution downstream of the fuel injector are essential for the development of viable high-speed combustors, since combustor stability, heat release rate, and combustion efficiency depends on local stoichiometry. The usual mode of introducing fuel into hypersonic engines is through one or more rows of discrete ports flush-mounted in the combustor walls or on intrusive injectors. The analytical model employed must be capable of assessing interactions that occur between injectant streams and the main airflow, the influence of approach flow boundary layer on jet penetration, and mutual interactions, which occur between adjacent ports.

During low-speed acceleration (i.e., ER and AAR modes of operation) and mode transition (i.e., AAR to RJ), fuel is injected into the combustor through secondary discrete ports (located on the base of the intrusive injectors and on the cowl and body surfaces of the combustor). Careful consideration must be given to the location of the secondary discrete ports of injectors to avoid impact on plume afterburning and combustor inlet interaction. At higher flight speeds (i.e., RJ and SJ mode of operation and mode transition) fuel is injected into the combustion zone through a set of discrete ports on the side of the intrusive injectors where fuel distribution can be tailored in a direction normal to airflow in the combustion zone. This allows the match of the fuel flow to the locally available airflow (thereby regulating the fuel flow from the secondary to primary injector ports) without combustor inlet interaction. Primary injector sizing and spacing is set to accommodate intrusive injector lateral distribution due to rocket integration, combustor entrance profiles, fuel staging, and variations in fuel properties along the described mission.

For X-43B, the fuel injection system is required to operate from flight Mach number 0.7 to 7.0. This range encompasses a wide variety of injection flow rates and locations. Furthermore, the fuel injector design is technically challenging because the wide range of fuel state properties caused by the significant variations in heat load to the combustor and endothermic reactions occurring in the heat exchanger of the engine. Particularly during AAR mode of operation the engine may develop substantial levels of heat load. However, during mode transition from AAR to RJ the heat load is reduced substantially. Consequently, the injector design must be capable of accommodating a wide range of momentum flux ratios, fuel temperatures, and molecular weight from 80 to 160 at the injector sites as the engine operates across the mission trajectory.

Methods for predicting the fuel distribution downstream of the fuel injector are essential for the generation of a viable combustor design, since thrust augmentation, combustor stability, heat release rate,

and combustion efficiency all depend on local stoichiometry. Primary objectives of the fuel-injector arrangement are to obtain a reasonably uniform combustible-fuel distribution across the combustor with minimal length requirements and pressure loss characteristics.

The analytical model employed must be capable of assessing interactions that occur between injectant streams and the main airflow, the turbulent mixing of fuel and air downstream of the injection station, the influence of approach flow boundary layer on jet penetration, and mutual interaction that occurs between adjacent ports. Numerous correlations have been developed to describe penetration trajectory as the stream-wise locus of points either outer boundary or peak concentration of jet. The correlation developed by Frederick P. Povinelli and Louis A. Povinelli is:¹⁷

Equation 2

$$\frac{y'}{d_j} = 3.21 \left(\frac{P_{o,j}}{P_{eb}} \right)^{0.416} M_j^{0.121} \left(\frac{x}{d_j} + 0.5 \right)^{0.203} \left(\frac{\theta}{d_j} \right)^{0.163}$$

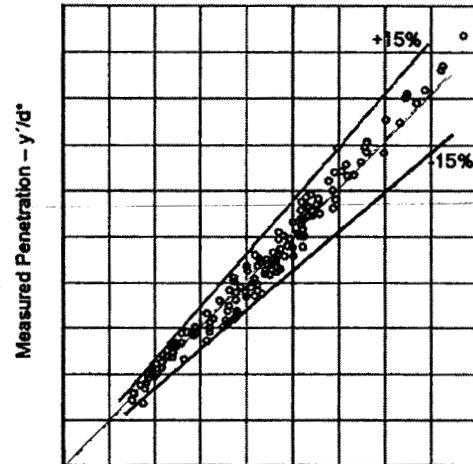
Where:

- y' is the penetration depth
- d_j is the injector or jet diameter
- $P_{o,j}$ is the injector supply pressure
- P_{eb} is the effective backpressure
- M_j is the jet Mach number
- x is the axial location
- θ is the core-flow momentum thickness.

For the purpose of clarity, the measured penetration plotted against the penetration calculated from Equation 2 results are presented in Figure 9, which was extracted from Reference 18, and shows excellent agreement between measured and calculated penetration (i.e., the agreement is within ± 15 percent for all data).

As a general practice, during the design and analysis process of airbreathing hypersonic propulsion systems, first order and FNS CFD numerical simulations are conducted sequentially. Mixing and combustion CFD simulations are substantiated by measured pressure distributions, calorimetric efficiency, and thrust measurements. Contour maps of air, fuel, and combustion product concentrations from a generic 3-D CFD simulation at a selected combustor axial location are illustrated in Figure 10. As seen in the combustor specie distributions of Figure 10, the selected fuel injector pattern and intrusive injector concept left *pockets* of unburned air on the cowl side of the combustor.

Further interrogation of the mixing and combustion CFD simulation near the fuel injector site provides significant insight into the fuel air distribution and penetration trajectory before and after combustion. Figure 11 presents the fuel mole fraction for the mixing and combustion CFD simulations. The fuel



$$\text{Calculated Penetration, } \frac{y'}{d_j} = 3.21 \left(\frac{P_{o,j}}{P_{eb}} \right)^{0.416} M_j^{0.121} \left(\frac{x}{d_j} + 0.5 \right)^{0.203} \left(\frac{\theta}{d_j} \right)^{0.163}$$

Figure 9. Comparison of Measured and Calculated Penetration for All Sets of Data with Boundary Layer Momentum Included in Correlation

concentration scale has been set from 5 percent (blue) to 10 percent (red) fuel mole fraction to emphasize the outer trajectory of the fuel. During the combustion process, the formation of precombustion shock in front and over the injector array changes the approach condition by increasing the momentum thickness and reducing the effective backpressure in the core. Consequently, the fuel achieves maximum penetration with combustion occurring sooner than the mixing-only case. The thick boundary layer from the precombustion shock shields the injected jet from the high momentum-free stream for a greater distance than a thin boundary layer. Reduced effective backpressure further improves the penetration level. Also note that the fuel tends to migrate upstream into the boundary layer of the precombustion shock.

Comparison of penetration height to jet diameter ratio as a function of distance to jet diameter ratio from Povinelli and Povinelli¹⁷ and CFD mixing and combustion is illustrated in Figure 12. The penetration trajectory with combustion is also presented in the Figure 12. It appears that Povinelli's correlation agrees well with the penetration trajectory from the mixing CFD simulation. The correlation over-predicts the penetration in the near field and under-predicts in the far field. However, in the far field they achieve similar penetration levels.

Combustor Thrust Potential and Engine I_{sp} Optimization

The ultimate measure of combustor performance is the engine thrust produced for specified combustor entrance conditions and equivalence ratio schedule. In a RBCC combustor configuration the available thrust potential at the combustor exit is reduced by the presence of intrusive injectors that contain the rocket thrusters (i.e., increased blockage and hence, drag). Other contributors to decrease

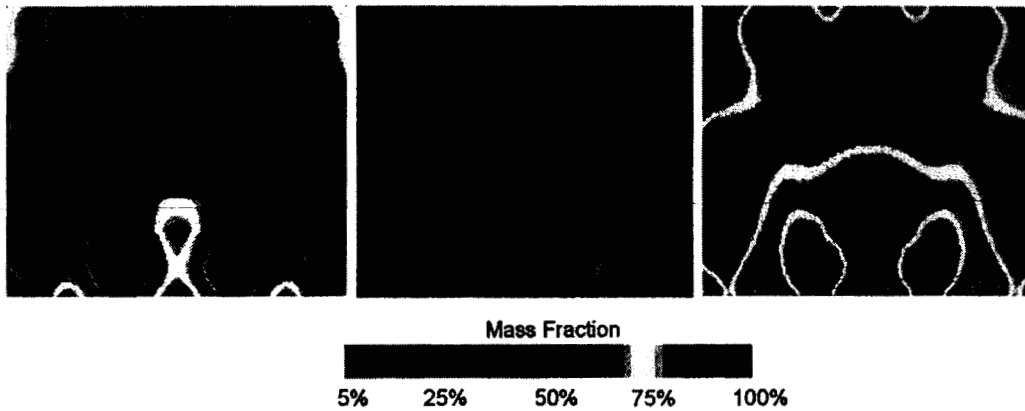


Figure 10. Air, Fuel, and Products of Combustion at Specified Axial Station

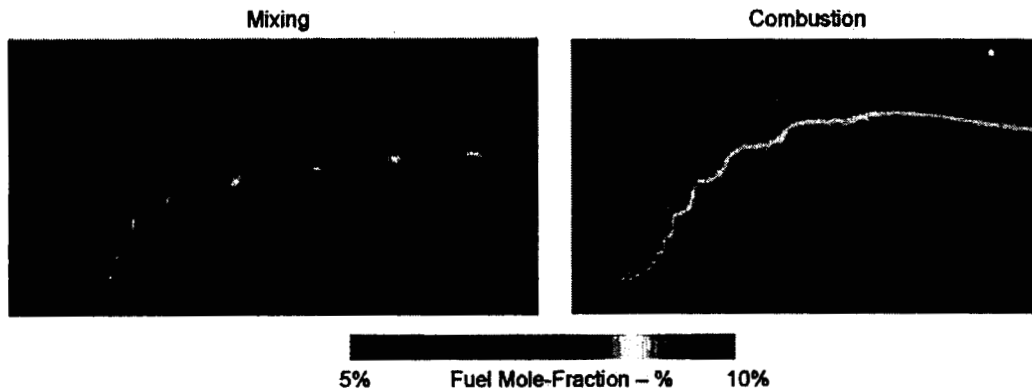


Figure 11. Fuel Penetration Trajectories

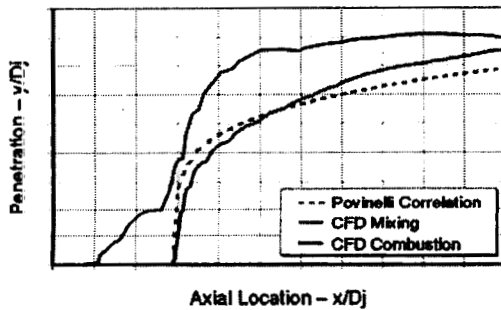


Figure 12. Comparison of Fuel Penetration Trajectories

thrust potential include mixing losses, wall heat transfer, and friction drag on the injectors and combustor walls.

Thrust potential analyses of injector/combustor designs completed to date use four processes: Taguchi-based orthogonal parameter matrices, CFD database, regression models, and performance cycle deck sensitivities. One approach is to establish a Net Thrust Differential (NTD) model using engine cycle performance sensitivity coefficients coupled with CFD base regression models. The NTD model can be used to evaluate thermally balanced engine performance and determine injector geometry and combustor length and will provide maximum engine

thrust and I_{sp} . An alternate approach is to incorporate the CFD-based regression model directly in the performance cycle deck to conduct parametrics on engine performance as a function of injector/combustor critical parameters. Both approaches require that the CFD-generated flowfield be one-dimensionalized using a scheme that conserves mass, momentum, and energy fluxes.^{18,19} The 1-D flow is expanded in an ideal or reference nozzle. The flow is expanded isentropically either to a fixed ratio or an ambient pressure generating net thrust potential.

Application of the thrust potential model to evaluate the effects of injector blockage on thrust at selected Mach numbers in the mission and combustor lengths is illustrated in Figure 13. The *Combustor-Thrust* curve presents the incremental improvement in thrust with mixing efficiency only. The *Injector/Combustor-Drag* curve presents the increase in drag resulting from increased injector blockage. The *Net Thrust* curve presents the resulting engine thrust obtained by subtracting effects *Injector/Combustor-Drag* from the thrust due to mixing. The best thrust solution is produced at injector blockage levels slightly lower than the best mixing resulting from the effects of drag. Figure 13 emphasizes the importance of considering both mixing and drag in the evaluation of injector performance. —

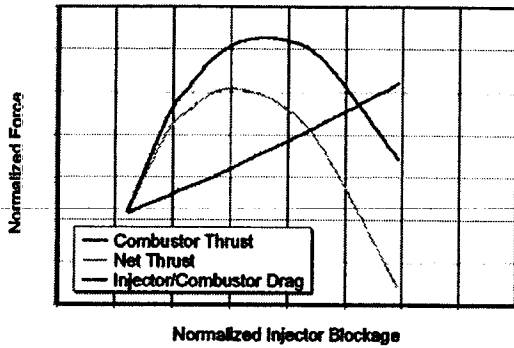


Figure 13. Intrusive Blockages Optimization Based on Thrust Potential

Effects of combustor length on engine thrust and I_{sp} at a specified flight Mach number are illustrated in Figure 14. In the near field, mixing and reaction dominates the process and hence, a rapid rise in thrust potential is observed. In the far field, combustion continues, however, the drag losses overcome the gain. The engine I_{sp} curve decreases more rapidly past the maximum resulting from increase of the combined effects of drag and heat load with combustor length. Optimum thrust and I_{sp} occurs at combustor lengths that end before mixing is completed. Figure 14 illustrates the necessity to design each component considering the entire system—not just the component efficiency.

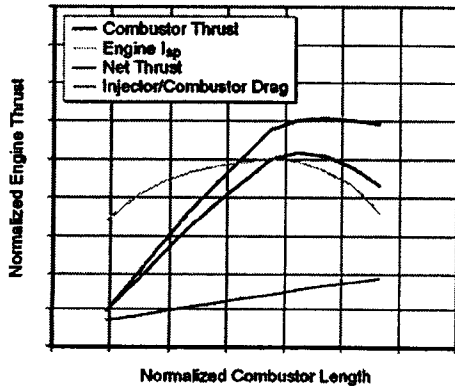


Figure 14. Combustor Length Optimization Based on Thrust and I_{sp}

Summary

This paper discussed highlights of the NASA MSFC ISTAR program with the focus on the design considerations of hydrocarbon fueled flowpath operating in AAR, RJ and SJ modes. The high level of integration required between vehicle and engine configuration is emphasized. The mission profile of the RBCC-powered X-43B was described, along with the hypersonic air-breathing RBCC propulsion modes of operation. Particular attention was focused on describing the requirements for, and the methods used in the multidisciplinary design process as the preferred injector/combustor configuration is devel-

oped. Critical design interactions occurring between various modes of operations were described.

The multidisciplinary design and optimization of an RBCC combustor requires simultaneous consideration of several key issues, as described in this paper. Proper accounting and consideration of losses in ejector modeling is key to accurate performance prediction and proper sizing and placement of rockets in the RBCC flowpath. First-order and 3-D FNS CFD analyses are essential to a successful design of a synergistic injector/combustor component operating over a wide range of flight conditions. The RBCC combustor must have sufficient base area to accommodate rocket integration flame stability with consideration to the injector drag characteristics at design Mach number. Primary fuel penetration and spreading considerations require minimum lateral rocket distribution to avoid excessive combustor length requirements. Careful consideration must be given to the location of the secondary discrete ports of injectors to avoid impact on plume afterburning and combustor inlet interaction. Geometric features of the RBCC combustor such as injector blockage and combustor length must be designed based on engine system-level requirements such as thrust potential and I_{sp} rather than individual component performance.

Acknowledgments

The ISTAR program is being performed by the RBC³ propulsion companies under NASA Contract Number NAS8-02001. Funding for this program is provided by the NASA MSFC, lead by Mr. J. Craig McArthur.

References

1. Faulkner, R.F., *Integrated System Test of an Airbreathing Rocket (ISTAR)*, AIAA 2001-1812.
2. Mack, G., C. Beaudry, A. Ketchum, *Integrated System Test of an Airbreathing Rocket (ISTAR)*, AAAF, May 14-16, 2002.
3. Hueter, Uwe., *Rocket-Based Combined Cycle Propulsion Technology for Access-to-Space Applications*, AIAA 1999-4925.
4. Huebner, L.D., K.E. Rock, E.G. Ruf, D.W. Witte, *HYPER-X Flight Engine Ground Testing For X-43 Flight Risk Reduction*, AIAA 2001-1809.
5. Kazmar, R.R., *Hypersonic Missile Propulsion System*, AIAA Paper, Nov 1999.
6. Faulkner, R.F., J.W. Weber, *Hydrocarbon Scramjet Propulsion System Development, Demonstration, and Application*, AIAA-99-4922.
7. Fortin, T.B., D.P. Wishart, D.G. Guinan, R. Norris, D. Modroukas, *Design, Manufacturing and Testing of an Actively Fuel-Cooled Scramjet Propulsion System*, AIAA-02-5252.

8. Hunt, J.L., C.R. McClinton, *Scramjet Engine/Airframe Integration*, AGARD-CP-600, Vol. 3: Sustained Hypersonic Flight, Paper C-35, 1997.
9. Quinn, J.E., *Oxidizer Selection for the ISTAR Program (Liquid Oxygen Versus Hydrogen Peroxide)*, AIAA-2002-4206.
10. McClinton, C.R., S.M. Ferelemann, K.E. Rock, P.G. Ferelemann, *The Role of Experiment Design in Hypersonic Flight System Technology Development*, AIAA-2002-0543.
11. Fabri, J., J. Paulton, *Theory and Experiments on Supersonic Air-to-Air Ejectors*, NACA-TM-91-1410.
12. Bernstein, A., W. Heiser, and C. Hevenor, *Compound Compressible Nozzle Flow*, AIAA-66-663.
13. Roan, V. P., *An Ejector Performance Correlation Factor*, AIAA-91-2545.
14. Winterfeld, G., *On Processes of Turbulent Exchange Behind Flameholders*, Tenth Symposium (International) on Combustion, pp. 1265-1275, The Combustion Institute, 1965.
15. Morrison C.Q., R.L. Campbell, R.B. Edelman, *Hydrocarbon Fueled Dual-Mode Ramjet/Scramjet Concept Evaluation*, ISABE-97-7053.
16. Ozawa, R.I., *Survey of Basic Data on Flame Stabilization and Propagation for High Speed Combustion Systems*, The Marquardt Co., Technical Report AFAPL-TR-70-81, January, 1971.
17. Povinelli, F.P., L.P. Povinelli, *Correlation of Secondary Sonic and Supersonic Gaseous Jet Penetration into Supersonic Crossflow*, NASA-TN-6370 June 1971.
18. Riggins, D.W., C.R. McClinton, *A Combustion Investigation of Flow Losses in Supersonic Combustor*, AIAA-90-2093.
19. Riggins, D.W., C.R. McClinton, *Analysis of Losses in Supersonic Mixing and Reacting Flow*, AIAA-91-2266.